AGU PUBLICATIONS

Geochemistry, Geophysics, Geosystems

RESEARCH ARTICLE

10.1002/2015GC005901

Key Points:
- Volcanic rocks in Sao Tome are Miocene in age by Ar/Ar dating
- Paleosecular variation is shown to be low at the equator
- Paleosecular variation is higher with higher latitude

Supporting Information:
- Supporting Information S1
- Table S1

Correspondence to:
N. D. Opdyke,
drno@ufl.edu

Citation:
Opdyke, N. D., D. V. Kent, D. A. Foster, and K. Huang (2015), Paleomagnetism of Miocene volcanics on Sao Tome: Paleosecular variation at the Equator and a comparison to its latitudinal dependence over the last 5 Myr, *Geochem. Geophys. Geosyst.*, *16*, 3870–3882, doi:10.1002/2015GC005901.

Received 5 MAY 2015
Accepted 10 OCT 2015
Accepted article online 14 OCT 2015
Published online 6 NOV 2015

Paleomagnetism of Miocene volcanics on Sao Tome: Paleosecular variation at the Equator and a comparison to its latitudinal dependence over the last 5 Myr

N. D. Opdyke[1], D. V. Kent[2,3], D. A. Foster[1], and K. Huang[1]

[1]Department of Geological Sciences, University of Florida, Gainesville, Florida, USA, [2]Department of Earth and Planetary Sciences, Rutgers University, Piscataway, New Jersey, USA, [3]Lamont-Doherty Earth Observatory of Columbia University, Palisades, New York, USA

Abstract A collection was made in January 2009 of 10 oriented samples from each of 54 sites in lavas on Sao Tome Island (nominal location 0.3°N, 6.5°E). Some sites were affected by lightning leaving a total of 42 sites for analysis of paleosecular variation. Overall magnetic properties were excellent (highly stable magnetizations carried by pseudosingle domain magnetite). After principal component analysis of progressive alternating field demagnetization data for the samples, 22 sites had normal polarity magnetizations ($D = 0.6°$, $I = -8.3°$, $\alpha_{95} = 4.3°$, $\kappa = 53.1$) and 20 had reverse magnetizations ($D = 176.0°$, $I = 4.2°$, $\alpha_{95} = 7.3°$, $\kappa = 20.8$); the directions are within 5° of antiparallel, yielding a positive reversal test. The combined data set of 42 site mean virtual geomagnetic poles converted to common (normal) polarity yields a pole position at 86.0°N, 211.5°E, $A_{95}=3.1°$. Ar/Ar and K/Ar dating reveals that these rocks are Miocene in age (~5–11 Ma), old enough to allow northerly plate motion to help explain the slightly far-sided pole position. The between-site dispersion in virtual geomagnetic poles was estimated as the angular standard deviation, S_b, and equaled 11.4° with 95% confidence interval between 9.9° and 13.4°.

1. Introduction

The time-averaged field initiative (TAFI) program [*Johnson et al.*, 2008] ended without new data being generated from within 15° of the Equator [*Lawrence et al.*, 2006], which is a critical region for understanding paleosecular variation of the geomagnetic field. Consequently, we undertook studies of the paleomagnetism of lava flows from equatorial regions in Ecuador (~0.6°S) [*Opdyke et al.*, 2006], Kenya (~0°, 2.6°N) [*Opdyke et al.*, 2010], and the Galapagos (~1°S) [*Kent et al.*, 2010]. The present study is an extension of these efforts.

Following sampling at Mt. Kenya and the reconnaissance collection from the Loiyangalani region [*Opdyke et al.*, 2010], we had planned to return to Loiyangalani the next year to collect more samples. However, public disorder in Kenya at the time prevented us from doing this, therefore we chose to sample lavas on Sao Tome in the Gulf of Guinea as an alternative site virtually on the Equator (Figure 1).

A paleomagnetic study of volcanics on Sao Tome was previously published by *Piper and Richardson* [1972]; they reported results from 49 sites using a least-scatter criterion on 2–5 samples per site that were subjected to progressive alternating field demagnetization. Other recent studies on volcanics in the region have been reported by *Ubangoh et al.* [1998] on mainland Cameroon and by *Herrero-Bervera et al.* [2004] on Mt. Cameroon, a study that is technically excellent but has only 10 sites reported. We therefore decided to resample and reanalyze the lavas on Sao Tome, which were thought to be Plio-Pleistocene (~0–5 Ma) in age.

2. Geology

Sao Tome Island is part of the Cameroon Volcanic Line. Pagalu is the last volcanic island in this chain and lies to the southwest of Sao Tome, which was constructed on oceanic crust [*Fitton and Dunlop*, 1985] (Figure 1). The volcanic rocks on the continent at the northeast end of the Cameroon trend are older and mainly Miocene and Oligocene in age. Mt. Cameroon, which is one of Africa's largest active volcanoes, is dominantly of Brunhes (middle and late Pleistocene) age and sits on continental crust near the current coastline [*Fitton and Dunlop*, 1985]. The origin of the volcanic rocks is a matter of debate and may be

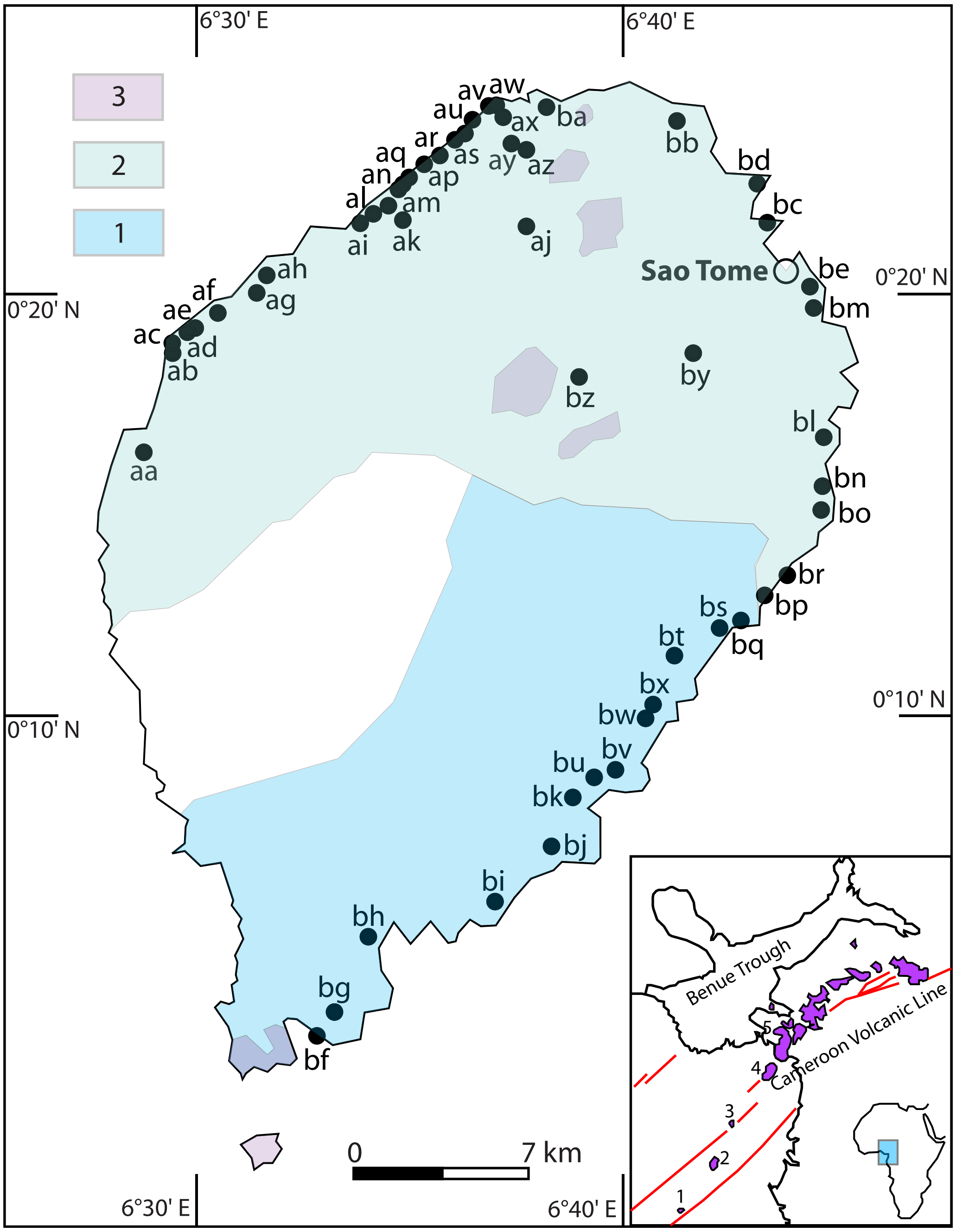

Figure 1. Site locations plotted on a preliminary geologic map of Sao Tome Island. The geology is following [*Caldeira and Munha*, 2002]. Legend: 1. basaltic lavas (3–8 Ma), 2. basaltic lavas (<1 Ma), and 3. Pyroclastic/lava cones (<0.4 Ma). The inset shows the regional geology and the volcanoes mentioned in the text: 1. Pagalu, 2. Sao Tome, 3. Principe, 4. Bioko, and 5. Mt. Cameroon.

plume-related, erupting along a previous fracture zone. The trend of the Cameroon line is parallel to the Benue trough [*Fitton and Dunlop*, 1985].

The geology of Sao Tome Island is dominated by outcrops of alkalic igneous rocks [*Caldeira and Munha*, 2002]. The extant radiometric dates indicate that lavas to the north of 0.15°N tend to be young (Late Pleistocene) and related to the modern volcano [*Barfod and Fitton*, 2014]. However, *Piper and Richardson* [1972] identified reverse polarity lavas in the area, indicating that lavas older than the Brunhes (>0.78 Ma) are present. Pyroclastic cones associated with scoriaceous flows are present in the northeastern part of the Island. The lavas in the southeastern part of the Island are dated as Miocene in age [*Fitton and Dunlop*, 1985]. Phonolite intrusions are present on the Island (Figure 1) and the lavas sometimes contain mantle-derived inclusions [*Caldeira and Munha*, 2002]. The result of our Ar/Ar dating (described below) indicates that most of the lavas currently exposed at sea level are Miocene in age (~5–11 Ma) even though younger lavas have been reported at higher elevations.

Lavas are exposed along the shoreline of Sao Tome along a beautiful paved road with fresh outcrops where blasting was used in road construction. Seaside exposures are abundant where the lavas are being actively eroded and not too badly weathered. Tracks branch off the highway to the coast or to plantations in the northern part of the Island. Jungle covers large areas of the central part of the island, which as a result is relatively inaccessible. Sampling was carried out mainly on roadside and beachfront outcrops using a hand-held gasoline-powered coring device with diamond bits which drilled cores 2.5 cm in diameter to a depth of 3 to 6 cm. Ten cores were drilled from each of 54 sites (outcrops). The cores were oriented using a Brunton compass and checked with a sun compass when possible. The sampling was carried out over several meters of outcrop to make certain that inadvertent sampling of a rolled boulder or outcrop struck by an isolated lightning strike would not wipe out the site. It was not possible in most cases to discern the stratigraphic relationship between sites (lavas) and in at least two cases in our study adjacent sites evidently sampled the same lava based on the coincidence of the directions.

3. Laboratory Studies

The samples were returned to the U.S. and processed in the Paleomagnetic Laboratory at the University of Florida. The samples were sliced into samples about 1cm thick. The natural remanent magnetization (NRM) of each sample was measured on a 2G cryogenic magnetometer and demagnetized using a commercially available alternating field (AF) demagnetizer. We have found that the most serious secondary overprint is caused by lightning strikes; therefore, progressive AF demagnetization was routinely employed because this hard overprint cannot be removed as effectively by thermal demagnetization.

Magnetic hysteresis curves to 1 Tesla were obtained from representative samples from all sites on a Micromag AGFM (Figure 2). The resulting plot of hysteresis parameter ratios (Figure 3) showed that the samples from Sao Tome fell predominately in the usual pseudosingle domain region with only one site in the single domain region and another near the multidomain region [*Day et al*., 1977].

The results of progressive AF demagnetization were analyzed using principal component line fitting [*Kirschvink*, 1980]. Three or more points were employed to determine the direction. If the line did not trend toward the origin, the sample was not included in the analysis. Demagnetization results for samples from four representative sites are shown in Figure 4. Three of the sample results (Figures 4a, 4c, 4d) are straightforward with linear demagnetization trajectories to the origin and shallow inclinations yielding both reverse polarity (southerly) and normal polarity (northerly) directions. Site aj (Figure 4b), however, exhibits scattered directions to the south and a separate cluster with steep negative inclinations. We interpret this to be an intermediate (transitional) direction. This is not surprising since both polarities are present in our data set. The paleomagnetic data from the near-multidomain site did not yield useable results.

Site-mean directions were calculated [*Fisher*, 1953] and are given in Table 1 and plotted in Figure 5. There are 22 normal polarity sites and 20 reverse polarity sites, for a total of 42 out of 54 sites that yield acceptable data. The normal sites are well grouped ($D = 0.6°$, $I = -8.3°$, $\alpha_{95} = 4.3°$, $\kappa = 53.1$) whereas the reverse sites are somewhat more dispersed ($D = 175°$, $I = 4.2°$, $\alpha_{95} = 7.3°$, $\kappa = 20.8$). The directions can be combined since the data pass a reversal test at a high confidence level (category A of *McFadden and McElhinny* [1990]). The overall statistics for 42 sites after inverting the reverse polarity site directions are $D=358.4°$, $I = -6.3°$, $\alpha_{95} = 4.1°$, $\kappa = 30.0$.

Virtual geomagnetic poles (VGPs) were calculated from the site-mean directions and are plotted in Figure 6. The mean VGP after inverting reverse polarity site directions is located at 86.0°N, 211.5°E, ($A_{95} = 3.1°$), which is just significantly different (far-sided) from the geographic axis. VGP dispersion was calculated using the method of *Cox* [1969] and yields an angular standard deviation, S_b of 11.4° with 95% confidence interval between 9.9° and 13.4°.

We can compare the results of this study to that of *Piper and Richardson* [1972]. It is rather amazing that the mean direction of our results ($D = 358.4°$, $I = -6.3°$) is within an insignificant 1° of their study ($D = 359.2°$, $I = -7.0°$). This shows clearly that older studies should not be rejected out of hand, especially for younger lavas.

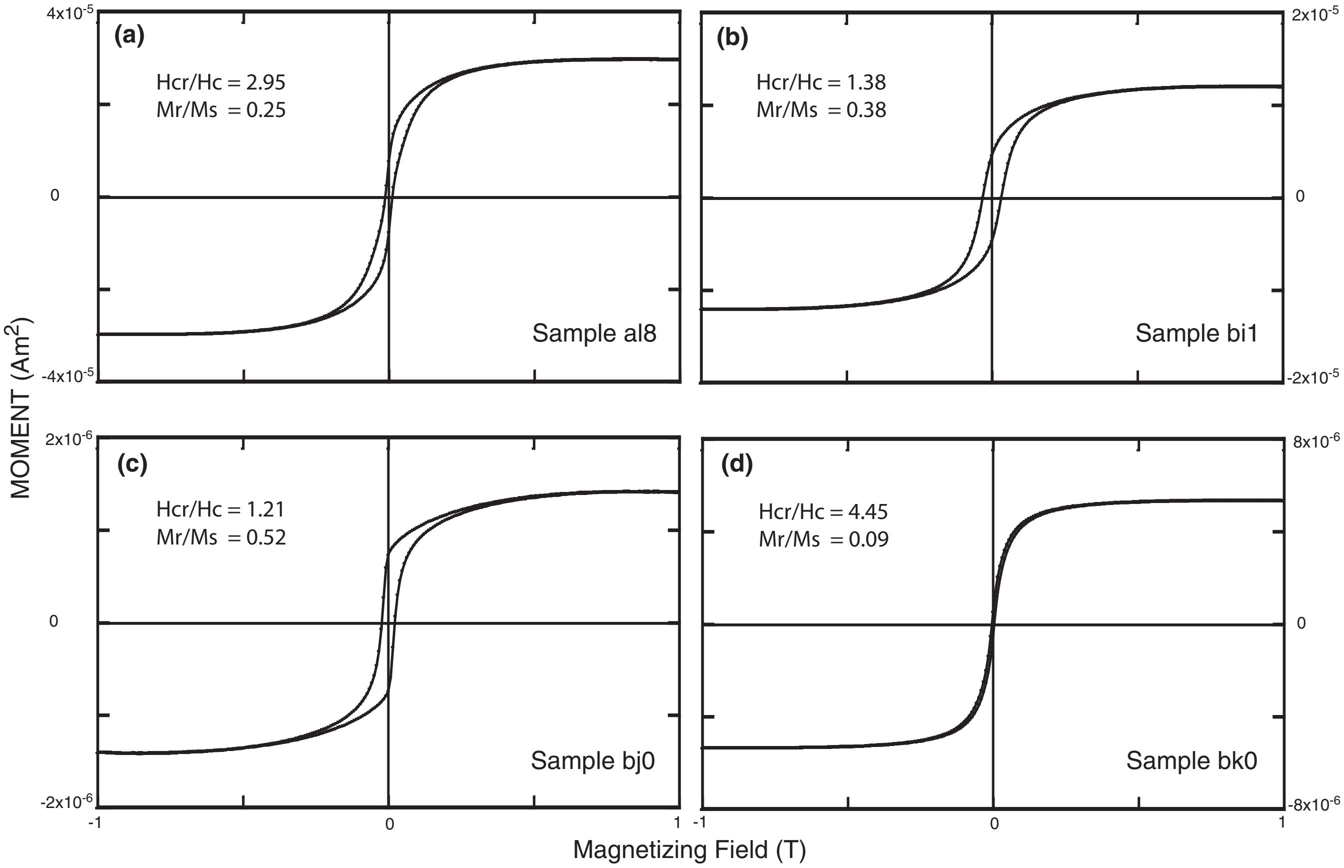

Figure 2. Magnetic hysteresis data from selected lava samples from sampling sites on Sao Tome.

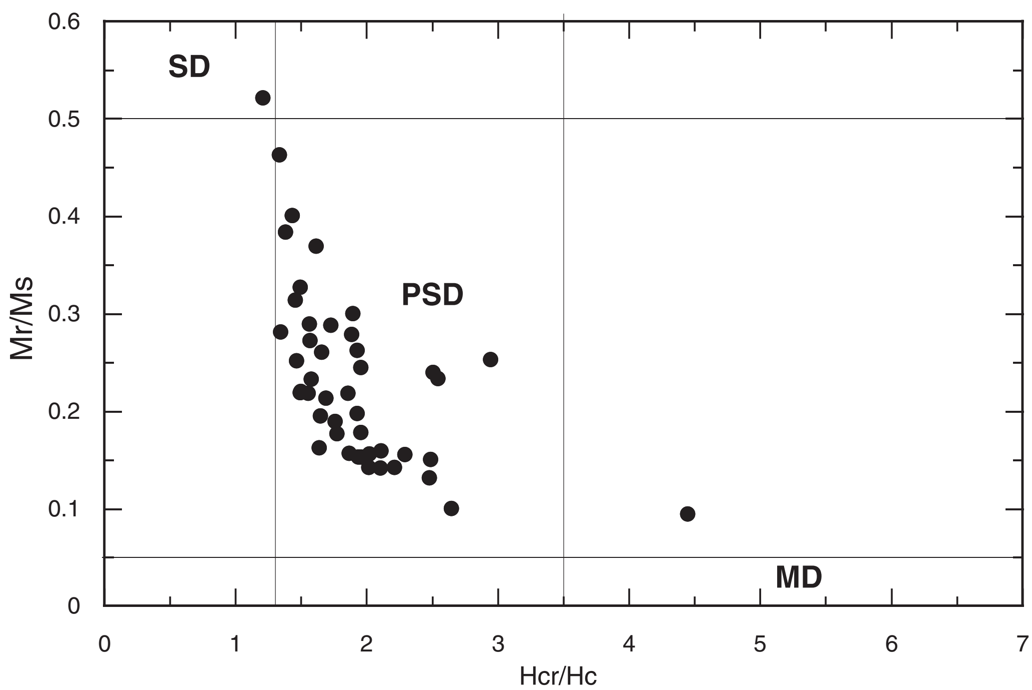

Figure 3. Day plot [*Day et al.*, 1977]. The majority of data from Sao Tome fall into the pseudosingle domain (PSD) region.

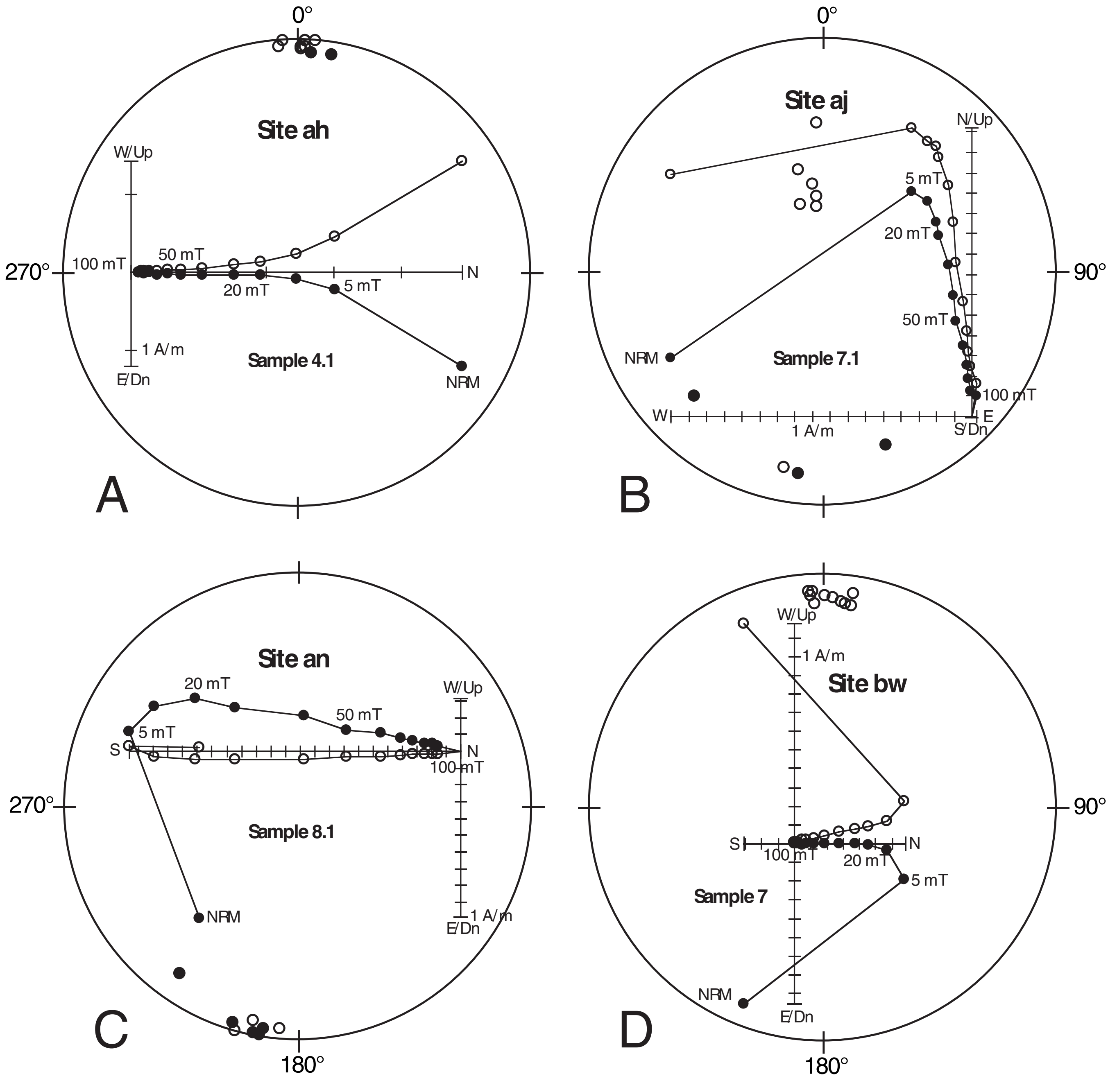

Figure 4. Representative vector endpoint diagrams from four Sao Tome sampling sites. ChRM directions from all samples from each of the site directions are also shown, giving an indication of site dispersion after demagnetization.

4. $^{40}Ar/^{39}Ar$ Data

Nine samples of selected lavas were analyzed in the $^{40}Ar/^{39}Ar$ laboratory at the University of Florida [*Foster et al*., 2009]. Fresh groundmass concentrates of the lavas weighing 50–200 mg were wrapped in Al-foil and loaded into a quartz glass tube along with 1 mg packages of the flux monitor GA1550 biotite. Flux monitor packages were placed between every two basalt samples in the quartz tubes. The samples and flux monitors were irradiated at the Oregon State reactor facility for 10 h. Samples were degassed using a double vacuum resistance furnace attached to a stainless steel extraction and cleanup line. Reactive gasses were removed with SAES getters prior to expansion to the mass spectrometer. Argon isotopes were analyzed using a MAP215-50 mass spectrometer with a Balzers electron multiplier. The data were reduced using

Table 1. Site Statistics for ChRM of Sao Tome Paleomagnetic Collection[a]

Site ID	P	Slon(E)	Slat	n	Dec	Inc	α_{95}	κ	Plon	Plat	A_{95}	K
		(E)	(N)		(°)	(°)	(°)		(°E)	(°N)	(°)	
aa	R	6°29.382′	0°18.528′	9	172.6	−0.5	5.1	102.2	96.3	−82.5	3.6	207.5
ab	N	6°29.382′	0°18.528′	10	356.9	−15.8	5.3	85.6	206.0	81.1	5.0	94.6
zac	N	6°29.379′	0°18.675′	8	3.6	−8.7	3.1	330.3	148.7	84.1	2.7	414.0
ad	N	6°29.379′	0°18.675′	10	355.6	−11.2	3.5	187.0	222.9	82.6	3.1	241.3
ae	N	6°30.008′	0°19.196′	6	9.3	3.7	5.7	140.5	86.8	80.6	4.4	233.1
af	N	6°30.491′	0°19.497′	10	351.8	7.7	5.2	87.1	300.0	81.0	4.4	122.8
ag	R	6°31.427′	0°20.013′	10	156.6	20.8	3.8	166.9	70.3	−64.2	3.3	212.6
ah	N	6°31.616′	0°20.404′	10	1.7	−0.7	3.4	206.5	116.9	88.2	2.6	342.5
ai	R	6°33.870′	0°21.645′	12	190.8	5.1	6.9	40.5	292.2	−78.8	4.8	83.2
ak+al	R	6°33.867′	0°21.763′	18	187.7	31.6	3.2	114.4	344.1	−70.8	2.8	157.4
am+an	R	6°34.519′	0°22.067′	18	195.4	2.2	4.2	68.0	282.0	−74.5	3.7	89.8
ao	R	6°34.825′	0°22.521′	10	175.8	−9.5	4.6	110.6	142.9	−83.9	3.8	165.9
ap	R	6°35.362′	0°23.052′	10	159.7	22.4	6.0	66.2	64.7	−66.4	5.1	91.2
aq	R	6°34.954′	0°22.612′	10	185.4	0.5	2.8	304.3	283.3	−84.6	2.3	459.9
ar	R	6°35.656′	0°23.276′	10	159.8	26.1	2.3	424.7	60.5	−65.5	2.0	569.4
as	R	6°36.078′	0°23.658′	10	179.5	1.1	2.9	282.1	36.1	−88.9	2.3	459.1
at	R	6°36.328′	0°23.845′	10	169.5	−14.2	3.0	268.3	129.8	−77.5	2.6	355.8
au	R	6°36.499′	0°24.154′	10	163.8	−6.3	3.3	221.8	106.4	−73.6	2.6	359.3
av	R	6°36.791′	0°24.404′	7	194.9	−5.1	9.1	45.4	268.0	−75.0	8.1	56.6
aw	R	6°36.912′	0°24.407′	10	187.7	−3.8	4.8	103.7	265.5	−82.1	3.5	189.5
ax	R	6°37.099′	0°24.194′	8	166.2	16.7	5.9	88.6	63.2	−73.5	4.9	130.5
az	N	6°37.735′	0°23.411′	10	353.1	−20.7	8.7	31.7	218.0	76.9	8.9	30.3
ba	N	6°38.257′	0°24.396′	9	359.4	−0.3	6.0	74.9	235.6	89.2	5.3	96.7
bb	R	6°41.248′	0°24.096′	10	177.7	5.4	5.9	69.0	43.4	−86.1	5.3	83.7
bc	N	6°43.429′	0°21.670′	10	5.9	−5.8	3.9	156.8	126.2	83.2	3.1	239.2
bd	N	6°43.156′	0°22.541′	10	0.7	−7.6	3.8	158.7	177.3	85.7	2.4	421.7
be	N	6°44.378′	0°20.099′	9	358.7	−3.7	7.0	55.2	217.3	87.5	6.1	72.9
bf	R	6°32.827′	0°02.289′	10	187.4	2.7	3.3	210.5	287.0	−82.5	2.8	298.0
bg	N	6°33.181′	0°01.919′	10	12.1	−24.1	3.6	176.4	143.7	72.6	3.2	223.5
bi	N	6°37.028′	0°05.511′	7	3.4	15.7	3.6	278.3	29.9	81.4	2.4	647.9
bj	R	6°38.280′	0°06.850′	10	165.8	−11.3	2.9	278.4	118.4	−74.7	2.4	393.0
bl	R	6°44.725′	0°16.599′	10	162.3	−6.6	2.9	280.6	107.0	−72.0	2.5	376.7
bm	R	6°44.510′	0°19.638′	10	177.9	5.6	6.4	58.4	39.9	−86.3	6.1	63.8
bn	N	6°44.621′	0°15.407′	10	358.4	−19.3	4.9	97.1	195.3	79.6	4.9	98.1
bo	N	6°44.694′	0°14.803′	9	349.9	−15.4	4.6	127.1	238.0	77.1	4.2	148.4
bp	N	6°43.340′	0°12.745′	10	2.4	−9.7	5.8	69.8	160.5	84.3	5.4	81.1
br	N	6°43.892′	0°13.250′	10	4.2	−8.6	5.4	82.0	143.9	83.8	5.1	89.2
bs	N	6°42.303′	0°11.995′	9	6.0	−5.6	4.4	137.4	150.8	79.9	3.3	248.5
bu	N	6°39.301′	0°08.473′	9	8.0	−10.6	1.9	711.9	131.4	80.4	1.6	1083.6
bw	N	6°40.552′	0°09.851′	10	1.8	−11.2	3.1	241.2	169.2	83.9	2.9	275.0
bx	N	6°40.681′	0°10.187′	6	359.3	−13.8	9.1	54.6	192.6	82.7	8.1	68.6
bz	N	6°38.969′	0°18.002′	10	350.2	−4.3	8.1	36.7	262.4	79.8	7.5	42.6
Normal	N	6.5°	0.3°	22	0.6	−8.3	4.3	53.1	179.5	85.5	3.0	110.6
Reversed	R	6.5°	0.3°	20	176.0	4.2	7.3	20.8	64.5	−85.1	5.8	32.9
Total	N+R	6.5°	0.3°	42	358.4	−6.3	4.1	30.0	211.5	86.0	3.1	50.7

[a]P = polarity with N = normal and R = reversed, Slon, Slat = site longitude and latitude, n = number of samples or sites used to calculate the mean directions, Dec, Inc = declination and inclination of the mean direction and α_{95}, κ = the associated 95% confidence circle radius and precision parameter, Plon, Plat = longitude and latitude of mean VGP and A_{95}, K = the associated 95% confidence circle radius and precision parameter. The VGP dispersion computed using *Cox*'s [1969] method is Sb = 11.4° with 95% confidence error range 9.9-13.4°.

ArArCALC [*Koppers*, 2002] and apparent ages were calculated using an age of 98.79 ± 0.96 Ma for the GA1550 biotite standard [*Renne et al*., 1998].

The analytical data for all nine samples are given in supporting information (Table S1). Age spectra diagrams are presented in Figure 7 and summary of the $^{40}Ar/^{39}Ar$ age results is given in Table 2. The samples gave $^{40}Ar/^{39}Ar$ ages ranging from about 5 to 11 Ma; all samples with Miocene $^{40}Ar/^{39}Ar$ ages are from the northeastern and around to the southern part of the island.

5. Dispersion of Earth's Magnetic Field and the Geocentric Axial Dipole

In order to understand the dispersion of the field with latitude, we have gathered together data from individual studies done within and outside of the TAFI program [*Johnson et al*., 2008]. The data were chosen on the following basis. With a few exceptions, the studies have at least five samples per site, which has been considered a minimum to provide reliable PSV information [*Tauxe et al*, 2003], and many studies have up to

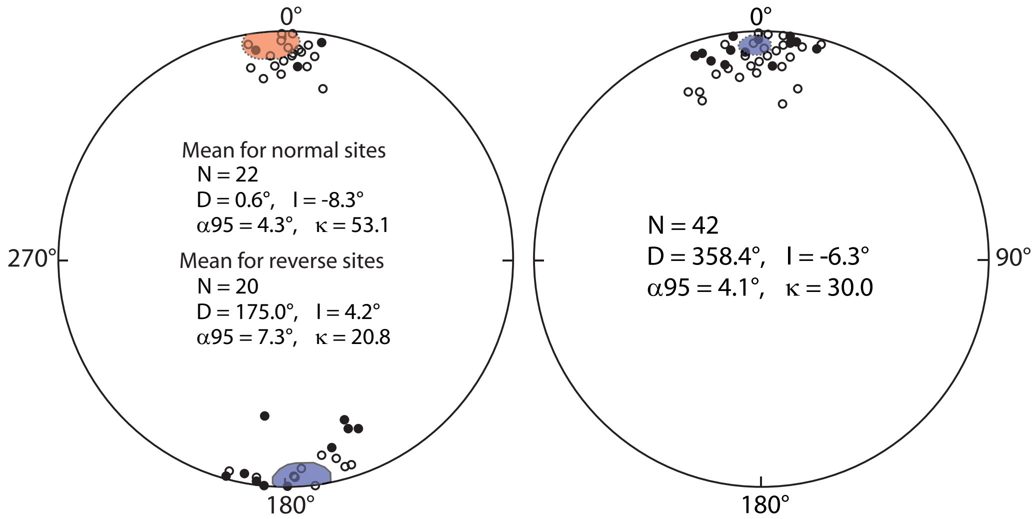

Figure 5. Site mean characteristic magnetizations plotted on a stereographic projection by site (left) and after inverting the directions of reverse polarity sites (right). Colored areas are 95% confidence circles around the mean directions.

10 samples per site, the number suggested originally in the TAFI protocol. As for the number of sites, *Tauxe et al.* [2003] suggested the more the better so we used at least 25 sites with samples that were thoroughly and progressively demagnetized and the directions determined from line fitting analysis. Sites with a 95% confidence circle radius greater than 10° were excluded and mean direction and pole were recalculated.

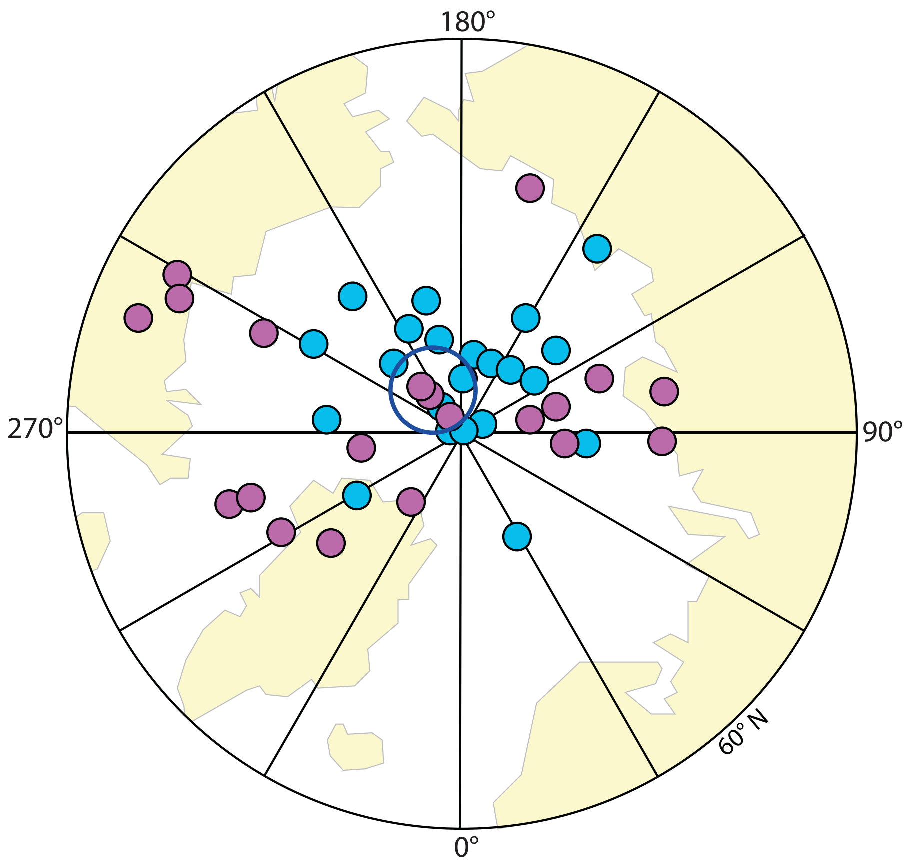

Figure 6. Virtual geomagnetic (north) pole positions plotted on an equal area polar projection. Blue circles are normal polarity site VGPs, red circles are inverted reverse polarity site VGPs. The circle of 95% confidence is plotted in blue for the overall mean VGP.

10.1002/2015GC005901

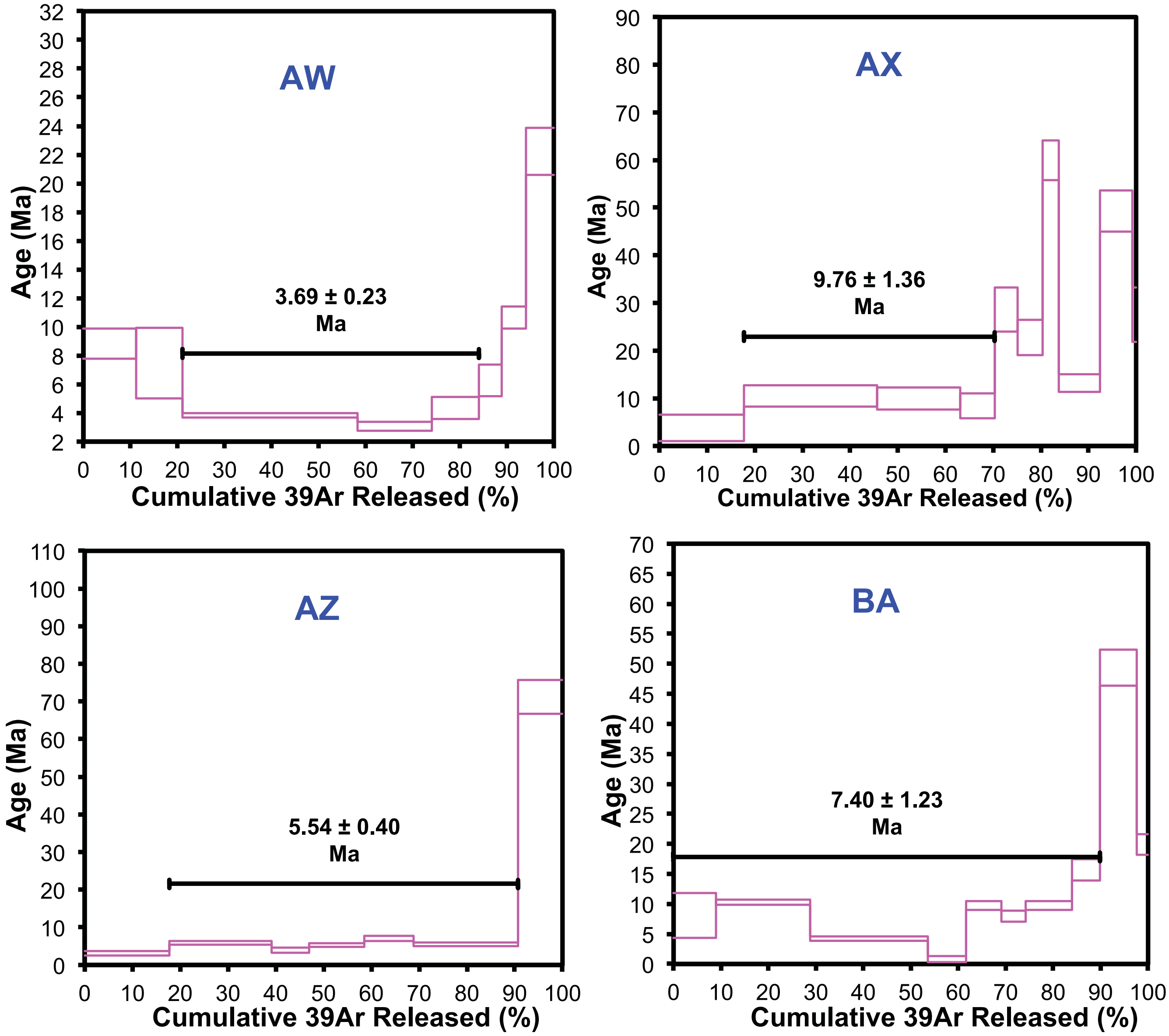

Figure 7. $^{40}Ar/^{39}Ar$ age spectra diagrams for ground mass concentrates of representative samples from Sao Tome.

Table 2. Summary of $^{40}Ar/^{39}Ar$ Data of Groundmass Concentrates

Sample	Age	Comment
aw	6.2 ± 0.3 Ma	Total fusion age
ax	9.8 ±01.4	Plateau age ~52% of the gas
az	5.4 ± 0.4 Ma	Plateau age >70% of the gas
ba	7.4 ± 1.2 Ma	Error plateau >90% of the gas
	11.2 ± 0.4 Ma	Total fusion age
bd	6.5 ± 1.5 Ma	Error plateau age
	14.1 ± 0.6 Ma	Total fusion age
be	10.4 ± 0.9 Ma	Plateau age >65% of gas; excess argon in plagioclase microphenocrysts
bi	9.0 ± 1.1 Ma	Total fusion age
bq	78.4 ± 4.3 Ma	Total fusion age, discordant spectrum
bs	47.3 ± 1.6 Ma	Total fusion age, discordant spectrum

Another issue is whether to include data from sites that may be associated with reversal transitions: we oppose combining transitional data with what can be ascribed to paleosecular variation. We believe that widely deviating transitional directions, such as the direction for site aj in this study (Figure 4b), should not be included in estimating paleosecular variation and the time-averaged field. We use a cut-off angle as proposed by *Vandamme* [1994].

Our database (Table 3) is composed of individual studies or in some cases combined nearby studies that are well-described and

Table 3. Compilation of Paleosecular Variation Parameters From Published Studies of 0–5 Ma Lavas[a]

ID[b]	Location	Slon (°E)	Slat (°N)	N	Dec (°)	Inc (°)	α_{95} (°)	Plon (°E)	Plat (°N)	K	A_{95} (°)	Sb (°)	Lb (°)	Ub (°)
1	Iceland	345.0	65.1	38	0.4	74.3	4.2	148.1	87.5	11.9	7.0	23.5	20.3	27.9
2	Nunivak	194.0	60.0	50	2.8	75.0	2.8	214.2	87.0	20.1	4.6	18.1	15.9	21.0
3	Aleutian	192.0	53.0	75	358.6	70.7	2.6	184.1	86.3	15.7	4.3	20.4	19.0	22.9
4	Br. Columbia	240.0	51.0	49	356.9	69.9	2.6	214.3	86.0	24.3	4.2	16.4	14.4	19.0
5	Eifel	7.0	50.3	32	7.0	68.6	3.2	67.6	85.1	27.5	4.9	15.4	13.2	18.6
6	Indian Heaven	238.3	46.0	56	2.6	65.2	2.5	270.0	87.3	28.7	3.6	15.1	13.4	17.4
7	Snake River	247.0	43.5	33	3.5	58.3	4.1	231.9	87.9	24.6	5.1	16.3	14.0	19.6
8	Sao Miguel	335.0	37.0	27	357.4	48.2	5.4	171.0	82.3	25.6	5.6	16.0	13.5	19.7
9	Pantelleria	13.0	37.0	39	5.3	50.9	3.1	154.9	83.3	43.4	3.5	12.3	10.6	14.5
10	Japan	136.0	36.0	53	357.6	51.9	3.5	3.9	87.5	27.4	3.8	15.5	13.7	17.9
11	San Francisco	248.2	35.4	54	355.7	53.8	3.1	150.6	86.1	30.8	3.5	14.6	12.9	16.8
12	Hawaii	202.2	21.3	118	1.4	28.1	2.2	5.7	84.1	53.5	1.8	11.1	10.2	12.2
13	Mexico	261.0	19.6	185	358.7	32.0	2.0	123.6	88.0	42.6	1.6	12.4	11.6	13.4
14	La Guadeloupe	298.3	16.0	25	0.5	30.2	4.1	348.0	89.3	63.1	3.7	10.2	8.6	12.6
15	Ethiopian Afar	41.5	12.0	61	2.5	16.9	3.8	177.9	86.5	42.6	2.8	12.4	11.0	14.2
16	Costa Rica	276.0	10.0	28	2.1	14.2	8.2	58.2	86.8	22.2	5.9	17.2	14.6	21.0
17	Kenya north	36.5	2.6	32	1.1	−1.0	4.1	197.6	86.5	77.1	2.9	9.2	7.9	11.1
18	Kenya south	36.5	0.0	69	0.7	−0.8	4.4	141.5	88.8	53.9	2.3	11.0	9.9	12.5
19	Ecuador	282.0	−0.6	51	359.9	−5.4	4.2	106.0	87.7	33.5	3.5	14.0	12.3	16.2
20	Galapagos	270.0	−1.0	61	357.0	1.2	3.0	207.8	86.6	70.8	2.2	9.6	8.6	11.0
21	Java	112.0	−7.4	35	359.6	−18.5	5.2	296.3	87.5	39.3	3.9	12.9	11.1	15.4
22	Society Is.	209.0	−17.0	116	1.2	−35.0	2.8	19.5	87.7	28.9	2.5	15.1	13.8	16.6
23	Easter Is.	250.8	−27.1	64	357.5	−44.8	2.5	164.1	87.5	43.1	2.7	12.3	11.0	14.0
24	Argentina	291.0	−36.0	31	357.3	−52.8	4.6	214.0	87.9	38.7	4.7	13.0	11.1	15.7
25	Victoria	143.5	−38.0	36	355.0	−57.9	6.7	25.5	86.2	26.6	4.7	15.7	13.5	18.7
26	New Zealand	176.0	−38.5	105	7.4	−58.4	2.1	284.9	84.1	27.1	2.7	15.5	14.2	17.2
27	Possession	51.8	−46.0	36	2.0	−64.0	3.7	165.2	88.7	20.4	5.4	17.9	15.4	21.3
28	Patagonia	290.0	−51.0	41	1.7	−67.8	3.6	72.5	88.8	18.5	5.3	18.8	16.3	22.2
29	Antarctica	166.0	−78.0	111	13.7	−80.7	3.4	207.5	84.7	12.4	4.0	23.0	21.0	25.4

[a]Slon, Slat = locality longitude and latitude, N = number of sites, Dec, Inc, α_{95} = declination, inclination and 95% confidence circle of the mean direction, Plon, Plat, K, A_{95} = longitude and latitude of the paleomagnetic pole and associated precision parameter and 95% confidence circle, Sb, lb, ub = VGP dispersion and its upper and lower bounds computed using *Cox*'s [1969] method. The data base was restricted to studies of the last 5 Ma using modern laboratory and analytical techniques; sites with α_{95} above 10° as well transitional sites using VGP cutoff method of *Vandamme* [1994] were excluded. Studies were often combined as indicated were often combined as indicated in data sources.

[b]Data source keyed to ID: 1. *Udagawa et.al.*, [1999]; 2. Coe, R. quoted in *Johnson et al.* [2008]; 3. *Stone and Layer* [2006]; 4. *Mejia et al.* [2002]; 5. *Bohnel et al.* [1982]; 6. *Mitchell et al.* [1989]; 7. *Tauxe et al.* [2004a] and *Mankinen* [2008]; 8. *Johnson et al.* [1998]; 9. *Zanella and Lanza* [1994], *Zanella et al.* [1999]; 10. *Tanaka and Kobayashi*, [2003]; 11. *Tauxe et al.* [2003] and *Mankinen* [2008]; 12. *Herrero-Bervera and Valet* [2002]; 13. *Mejia et al.* [2005]; 14. *Carlut et al.* [2000]; 15. *Acton et al.* [2000] and *Kidane et al.* [2003]; 16. *Cromwell et al.* [2013]; 17, *Opdyke et al.* [2010]; 18, Recalculated from *Opdyke et al.* [2010]; 19. *Opdyke et al.* [2006]; 20. *Kent et al.* [2010]; 21. *Elmaleh et al.* [2004]; 22. *Yamamoto et al.* [2002]; 23. *Brown* [2002] and *Miki et al.* [1998]; 24. *Quidelleur et al.* [2009]; 25. *Opdyke and Musgrave* [2004]; 26. *Tanaka et al.* [1996, 1997, 2009]; 27. *Camps et al.* [2001]; 28. *Mejia et al.* [2004]; 29. *Tauxe et al.* [2004b] and *Lawrence et al.* [2009].

documented, for example, the results from Easter Island by *Miki et al.* [1998] and *Brown* [2002]. We do this to increase N to acceptable levels (N > 25 sites). However, we also believe that some studies are able to stand alone, such as Indian Heaven in Washington State (USA) by *Mitchell et al.* [1989]. The best analyses are from very large studies like the results from Mt. Kenya [*Opdyke et al.*, 2010]. In certain cases, there are many sites but the quality is indifferent; for example, most sites in the studies on Iceland have fewer than five samples per site. Iceland is the place where the geocentric axial dipole field was first calculated from lava results [*Hospers*, 1951] yet some studies on lavas from Iceland do not average to the GAD. The study chosen to represent Iceland was done by *Udagawa et al* [1999], trying to replicate a study by *Watkins et al.* [1977] that purportedly found a normal polarity site they named the Gilsa Event.

The angular dispersion of VGPs, estimated as the between-site angular standard deviation (Sb) [*McElhinny and Merrill*, 1975], from the database studies (Table 3) is plotted against collection latitude in Figure 8a. Latitudinal dependence in angular dispersion has long been observed in the modern geomagnetic field and in paleomagnetic data and described by various models [*Cox*, 1970; *McElhinny and Merrill*, 1975]. We have shown earlier [*Opdyke et al.*, 2010] that VGP dispersion is indeed low at the equator whereas data from Antarctica in high southern latitudes as well as from Iceland and Nunivak Island in high northern latitudes have higher dispersion. High-quality results from low latitudes have become more abundant in recent years and are an extension of the TAFI project. These studies include those based on samples that were collected in the past and have been taken from storage and reprocessed using modern methodology [*Grommé et al.*, 2010; *Kent et al.*, 2010], other studies on more recently collected and analyzed samples [*Opdyke et al.*, 2006; *Opdyke et al.*, 2010; *Johnson et al.*, 2008], and some older studies that are well done. Altogether there are

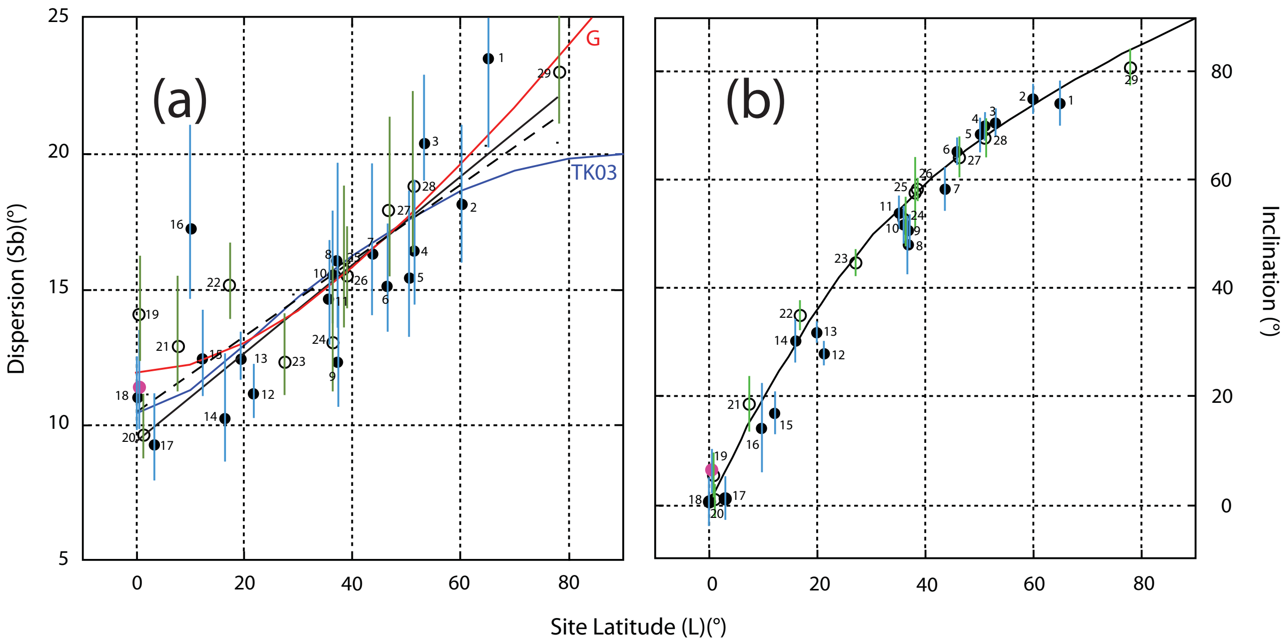

Figure 8. VGP dispersion Sb (a) and mean Inclination (b) plotted versus absolute site latitude (L) for PSV studies keyed to Table 3. Linear regression of Sb versus L is shown by straight lines in Figure 8a: the dashed line is computed by including the data from Costa Rica (#16) and Ecuador (#19) and is described by $Sb=10.477+0.140$ L, R = 0.814; the solid line is computed by excluding them and described by $Sb=9.351+0.161$ L, R = 0.890. Curves for Model G [*McElhinny and McFadden*, 1997] (red) and TK03 [*Tauxe and Kent*, 2004] (blue) are also shown for comparison. Curve for Inclination, I, versus latitude, L, according to dipole formula (tan I = 2 Tan L) is shown in Figure 8b. Solid (open) circles denote study areas in northern (southern) hemisphere.

now seven (including Sao Tome) studies that meet modern standards (Table 3) that were sampled within 10° of the equator. The VGP dispersion (S_b) is in general low, less than 13° (although two studies have somewhat higher dispersions for possible reasons discussed below: from Ecuador, $S_b = 14.0°$ and Costa Rica, $S_b = 17.2°$). The average value of S_b obtained by *McElhinny and McFadden* [1997] for the bin from 0 to ±10° latitude is 11.7°, which is similar to the value obtained in our analysis: Sb = 12.5° for seven studies within 10° of the Equator, or $S_b = 11.3°$ for five studies excluding the anomalously high S_b from Ecuador and Costa Rica (Table 3). It should be emphasized that the data sets in these two studies are independent—ours based on specific studies by locality, theirs [*McElhinny and McFadden* [1997] on grouping then-available sites in latitude bands—and the two studies support one another. The conclusion is that the true value of S_b at equatorial latitudes is low compared to higher latitudes as emphasized by *McElhinny and McFadden* [1997]. From the data presented here from Sao Tome, especially in comparison to the higher VGP scatter from the middle to late Miocene Columbia River Basalts at about 46°N latitude [*Dominguez and Van der Voo*, 2014], this seems to be true for the Miocene as well.

A least squares linear fit to S_b as a function of latitude (Figure 8a), with or without the inclusion of data from Costa Rica and Ecuador, agrees with Model G of *McElhinny and McFadden* [1997]. Also shown for comparison is a curve for Model TK03 [*Tauxe and Kent*, 2004]. At high latitudes, only Model G gives a satisfactory fit to the very sparse data there, even though TK03 was actually tuned to the underlying data for Model G. In any case, the data plotted in Figure 8a and listed in Table 3 effectively eliminate models of PSV that are invariant with latitude such as the Giant Gaussian Process model of *Constable and Parker* [1988] [e.g., see *Tauxe and Kent*, 2004, Figure 2].

6. Discussion

The data presented here agree with a paleomagnetic field that is predominantly dipolar, as shown in Figure 8b, although a small (few percent) contribution from an axial quadrupole field [e.g., *Carlut and Courtillot*, 1998] is certainly possible. There is also a basic axial symmetry in the paleosecular variation data, which is imposed by the GAD field. Until the database is improved, it is difficult to be certain that the symmetry

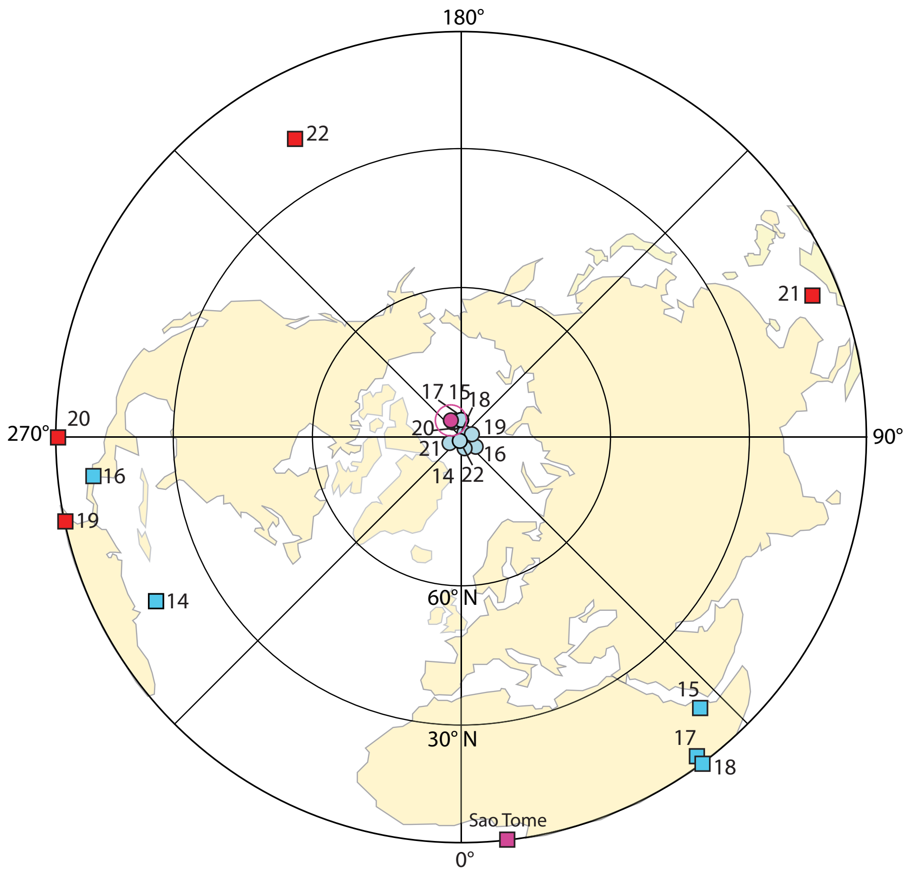

Figure 9. Equal area projection showing sampling localities in the equatorial (squares, blue in northern hemisphere, red projected from southern hemisphere) along with corresponding paleomagnetic poles (circles) for studies keyed to Table 3. The poles from these studies are generally close to the axis of rotation although the paleomagnetic pole from this study (star) is far-sided and the circle of confidence just misses the axis of rotation.

along lines of latitude is global. We show here that at least the data from equatorial latitudes is not asymmetric (Figure 9) although an increase in Pacific data would be desirable.

As mentioned above, the results from Ecuador and Costa Rica show higher dispersion than expected on the basis of the other results. This is mostly likely due to the tectonic setting rather than a true measure of the actual geomagnetic dispersion. Both studies are set in actively deforming regions and along a convergent plate boundary and therefore prone to tilting. In the early stages of studies of paleosecular variation, oceanic islands were the preferred collecting localities [e.g., *Cox*, 1971; *Doell and Cox*, 1971; *Watkins et al*., 1972]. To make more progress in the future, restudy of many of these islands should be attempted and areas of active tectonism (e.g., arc volcanoes) should be avoided.

Acknowledgments
We wish to express our thanks to the National Science Foundation for funding this study in Kenya (EAR0608998 to N.D.O. and EAR0609339 to D.V.K.). We would like to thank the Government of Sao Tome to allow us to collect samples and to ship them to the United States. The data presented in this paper can be accessed through the journal or the authors. Lamont-Doherty Earth Observatory contribution 7940.

References

Acton, G. D., A. Tessema, M. Jackson, and R. Bilham (2000), The tectonic and geomagnetic significance of paleomagnetic observations from volcanic rocks from central Afar, Africa, *Earth Planet. Sci. Lett.*, *180*, 225–241.

Barfod, D. N., and J. G. Fitton (2014), Pleistocene volcanism on São Tomé, Gulf of Guinea, West Africa, *Quat. Geochronol.*, *21*, 77–89.

Bohnel, H., H. Kohnen, J. Negendank, and H. Schmincke (1982), Paleomagnetism of Quaternary volcanics of the East-Eifel, Germany, *J. Geophys.*, *51*(1), 29–37.

Brown, L. (2002), Paleosecular variation from Easter Island revisited: Modern demagnetization of a 1970s data set, *Phys. Earth Planet. Int.*, *133*, 73–81.

Caldeira, R., and J. M. Munha (2002), Petrology of ultramafic nodules from Sao Tome Island, Cameroon Volcanic Line (oceanic sector), *J. Afr. Earth Sci.*, *34*, 231–246.

Camps, P., B. Henry, M. Prevot, and L. Faynot (2001), Geomagnetic paleosecular variation recorded in Plio-Pleistocene volcanic rocks from Possession Island (Crozet Archipelagol, southern Indian Ocean), *J. Geophys. Res.*, *106*, 1961–1971.

Carlut, J., and V. Courtillot (1998), How complex is the time-averaged geomagnetic field over the past 5 Myr?, *Geophys. J. Int.*, *134*, 527–544.

Carlut, J., X. Quidelleur, V. Courtillot, and G. Boudon (2000), Paleomagnetic directions and K/Ar dating of 0 to 1 Ma lava flows from La Guadeloupe Island (French West Indies): Implications for time-averaged field models, *J. Geophys. Res.*, *105*, 835–849.

Constable, C. G., and R. L. Parker (1988), Statistics of the geomagnetic secular variation for the past 5 m.y., *J. Geophys. Res.*, *93*, 11,569–11,581.

Cox, A. (1969), Confidence limits for the precision parameter κ, *Geophys. J. R. Astron. Soc.*, *18*, 545–549.

Cox, A. (1970), Latitude dependence of the angular dispersion of the geomagnetic field, *Geophys. J. R. Astron. Soc.*, *20*, 253–269.

Cox, A. (1971), Paleomagnetism of San Cristobal Island, Galapagos, *Earth Planet. Sci. Lett.*, *11*, 152–160.

Cromwell, G., C. G. Constable, H. Staudigel, L. Tauxe, and P. Gans (2013), Revised and updated paleomagnetic results from Costa Rica, *Geochem. Geophys. Geosyst. 14*, 3379–3388, *doi*:10.1002/ggge.20199.

Day, R., M. Fuller, and V. A. Schmidt (1977), Hysteresis properties of titanomagnetites: Grain-size and compositional dependence, *Phys. Earth Planet. Int.*, *13*, 260–267.

Doell, R. R., and A. Cox (1971), Pacific geomagnetic secular variation, *Science*, *171*(3968), 248–254.

Dominguez, A. R., and R. Van der Voo (2014), Secular variation of the middle and late Miocene geomagnetic field recorded by the Columbia River Basalt Group in Oregon, Idaho and Washington, USA, *Geophys. J. Int.*, *197*(3), 1299–1320.

Elmaleh, A., J. P. Valet, X. Quidelleur, A. Solihin, H. Bouquerel, T. Tesson, E. Mulyadi, A. Khokhlov, and A. D. Wirakusumah (2004), Palaeosecular variation in Java and Bawean Islands (Indonesia) during the Brunhes chron, *Geophys. J. Int.*, *157*, 441–454.

Fisher, R. A. (1953), Dispersion on a sphere, *Proc. R. Soc. London*, *A217*, 295–305.

Fitton, J. G., and H. M. Dunlop (1985), The Cameroon line, West Africa, and its bearing on the origin of oceanic and continental alkali basalt, *Earth Planet. Sci. Lett.*, *72*(1), 23–38.

Foster, D. A., B. D. Goscombe, and D. R. Gray (2009), Rapid exhumation of deep crust in an obliquely convergent orogen: The Kaoko Belt of the Damara Orogen, *Tectonics*, *28*, TC4002, doi:10.1029/2008TC002317.

Grommé, C. S., E. A. Mankinen, and M. Prévot (2010), Time-averaged paleomagnetic field at the equator: Complete data and results from the Galapagos Islands, Ecuador, *Geochem. Geophys. Geosyst.*, *11*, Q11009, doi:10.1029/12010GC003090.

Herrero-Bervera, E., and J.-P. Valet (2002), Paleomagnetic secular variation of the Honolulu Volcanic Series (33–700 ka), O'ahu (Hawaii), *Phys. Earth Planet. Int.*, *133*, 83–97.

Herrero-Bervera, E., R. Ubangoh, F. T. Aka, and J.-P. Valet (2004), Paleomagnetic and paleosecular variation study of the Mt. Cameroon volcanics (0.0-0.25 Ma), Cameroon, West Africa, *Phys. Earth Planet. Int.*, *147*(2-3), 171–182.

Hospers, J. (1951), Remanent magnetism of rocks and the history of the geomagnetic field, *Nature*, *168*, 1111–1112.

Johnson, C. L., J. R. Wijbrans, C. G. Constable, J. Gee, H. Staudigel, L. Tauxe, V. H. Forjaz, and M. Salgueiro (1998), 40Ar/39Ar ages and paleomagnetism of Sa'o Miguel lavas, Azores, *Earth Planet. Sci. Lett.*, *160*, 637–649.

Johnson, C. L., et al. (2008), Recent investigations of the 0–5 Ma geomagnetic field recorded by lava flows, *Geochem. Geophys. Geosyst.*, *9*, Q04032, doi:10.1029/02007GC001696.

Kent, D. V., H. Wang, and P. Rochette (2010), Equatorial paleosecular variation of the geomagnetic field from 0-3 Ma lavas from the Galapagos Islands, *Phys. Earth Planet. Int.*, *183*, 404–412.

Kidane, T., V. Courtillot, I. Manighetti, L. Audin, P. Lahitte, X. Quidelleur, P.-Y. Gillot, Y. Gallet, J. Carlut, and T. Haile (2003), New paleomagnetic and geochronologic results from Ethiopian Afar: Block rotations linked to rift overlap and propagation and determination of a ~2 Ma reference pole for stable Africa, *J. Geophys. Res.*, *108*(B2), 2102, doi:10.1029/2001JB000645.

Kirschvink, J. L. (1980), The least-squares line and plane and the analysis of palaeomagnetic data, *Geophys. J. R. Astron. Soc.*, *62*, 699–718.

Koppers, A. A. P. (2002), ArArCALC: Software for Ar-40/Ar-39 age calculations, *Comput. Geosci.*, *28*(5), 605–619.

Lawrence, K. P., C. G. Constable, and C. L. Johnson (2006), Paleosecular variation and the average geomagnetic field at ± 20° latitude, *Geochem. Geophys. Geosyst.*, *7*, Q07007, doi:10.1029/02005GC001181.

Lawrence, K. P., L. Tauxe, H. Staudigel, C. Constable, A. Koppers, W. McIntosh, and C. L. Johnson (2009), Paleomagnetic field properties at high southern latitude, *Geochem. Geophys. Geosyst.*, *10*, Q01005, doi:10.1029/02008GC002072.

Mankinen, E. A. (2008), Paleomagnetic study of late Miocene through Pleistoene igneous rocks from the southwestern USA: Results from the historic collections of the US. Geological Survey Menlo Park laboratory, *Geochem. Geophys. Geosyst.*, *9*, Q05017, doi:10.1029/02008GC001957.

McElhinny, M. W., and P. L. McFadden (1997), Paleosecular variation over the past 5 Myr based on a new generalized database, *Geophys. J. Int.*, *131*, 240–252.

McElhinny, M. W., and R. T. Merrill (1975), Geomagnetic secular variation over the past 5 m.y., *Rev. Geophys. Space Phys.*, *13*, 687–708.

McFadden, P. L., and M. W. McElhinny (1990), Classification of the reversal test in palaeomagnetism, *Geophys. J. Int.*, *103*, 725–729.

Mejia, V., R. W. Barendregt, and N. D. Opdyke (2002), Paleosecular variation of Brunhes age lava flows from British Columbia, Canada, *Geochem. Geophys. Geosyst.*, *3*(12), 8801, doi:10.1029/2002GC000353.

Mejia, V., N. D. Opdyke, J. F. Vilas, B. S. Singer, and J. S. Stoner (2004), Plio-Pleistocene time-averaged field in southern Patagonia recorded in lava flows, *Geochem. Geophys. Geosyst.*, *5*, Q03H08, doi:10.1029/2003GC000633.

Mejia, V., H. Bohnel, N. D. Opdyke, M. A. Ortega-Rivera, J. K. W. Lee, and J. J. Aranda-Gomez (2005), Paleosecular varation and time-averaged field recorded in late Pliocene-Holocene lava flows from Mexico, *Geochem. Geophys. Geosyst.*, *6*, Q07H19, doi:10.1029/2004GC000871.

Miki, M., S. Inokuchi, S. Yamaguchi, J. Matsuda, N. Nagao, N. Isezaki, and K. Yaskawa (1998), Geomagnetic paleosecular variation in Easter Island, the southeast Pacific, *Phys. Earth Planet. Int.*, *129*, 205–243, doi:10.1016/S0031-9201(1097)00106-00104.

Mitchell, R. J., D. J. Jeager, J. F. Diehl, and P. E. Hammond (1989), Paleomagnetic results from the Indian Heaven volcanic field, southcentral Washington, *Geophys. J. R. Astron. Soc.*, *97*, 381–390.

Opdyke, N. D., and R. Musgrave (2004), Paleomagnetic results from the newer volcanics of Victoria: Contribution to the time averaged field initiative, *Geochem. Geophys. Geosyst. 5*, Q03H09, doi:10.1029/2003GC000632.

Opdyke, N. D., M. Hall, V. Mejia, K. Huang, and D. A. Foster (2006), The time averaged field at the equator: Results from Ecuador, *Geochem. Geophys. Geosyst.*, *7*, Q11005, doi:10.11029/12005GC001221.

Opdyke, N. D., D. V. Kent, K. Huang, D. A. Foster, and J. P. Patel (2010), Equatorial paleomagnetic time averaged field results from 0-5 Ma lavas from Kenya and the latitudinal variation of angular dispersion, *Geochem. Geophys. Geosyst.*, *11*, Q05005, doi:10.1029/02009GC002863.

Piper, J. D. A., and A. Richardson (1972), The paleomagnetism of the Gulf of Guinea volcanic province, West Africa, *Geophys. J. R. Astron. Soc.*, *29*, 147–171.

Quidelleur, X., J. Carlut, P. Tchilinguirian, A. Germa, and P. Y. Gillot (2009), Paleomagnetic directions from mid-latitude sites in the southern hemisphere (Argentina): Contribution to time averaged field models, *Phys. Earth Planet. Int.*, *172*(3–4), 199–209.

Renne, P. R., C. C. Swisher, A. L. Deino, D. B. Karner, T. L. Owens, and D. J. DePaolo (1998), Intercalibration of standards, absolute ages and uncertainties in Ar-40/Ar-39 dating, *Chem. Geol.*, *145*(1–2), 117–152.

Stone, D. B., and P. W. Layer (2006), Paleosecular variation and GAD studies of 0-2 Ma flow sequences from the Aleutian Islands, Alaska, *Geochem. Geophys. Geosyst.*, *7*, Q04H22, doi:10.1029/2005GC001007.

Tanaka, H., and T. Kobayashi (2003), Paleomagnetism of the late quaternary ontake volcano, Japan: Directions, intensities, and excursions, *Earth Planets Space*, *55*, 189–202.

Tanaka, H., G.M. Turner, B.F. Houghton, T. Tachibana, M. Kono and M.O. McWilliams (1996), Palaeomagnetism and chronology of the central Taupo Volcanic Zone, New Zealand, *Geophys. J. Int.*, *124*, 919–934.

Tanaka, H., K. Kawamura, K. Nagao, and B. F. Houghton (1997), K-Ar ages and paleosecular variation of direction and intensity from quaternary lava sequences in the Ruapehu volcano, New Zealand, *J. Geomagn. Geoelectr.*, *49*(4), 587–589.

Tanaka, H., N. Komuro and G.M. Turner (2009), Palaeosecular variation for 0.1-21 Ka from the Okataina Volcanic Centre, New Zealand, *Earth Planets Space*, *61*, 213–225.

Tauxe, L., and D. V. Kent (2004), A simplified statistical model for the geomagnetic field and the detection of shallow bias in paleomagnetic inclinations: Was the ancient magnetic field dipolar?, in *Timescales of the Paleomagnetic Field, Geophys. Monogr.,145*, edited by J. E. T. Channell et al., pp. 101–116, AGU, Washington, D. C.

Tauxe, L., C. Constable, C. L. Johnson, A. A. P. Kopper, W. R. Miller, and H. Staudigel (2003), Paleomagnetism of the southwestern U.S.A. recorded by 0-5 Ma igneous rocks, *Geochem. Geophys. Geosyst.*, *4*(4), 8802, doi:10.1029/2002GC000343.

Tauxe, L., P. Gans, and A. Mankinen (2004a), Paleomagnetism and Ar/Ar ages from volcanics extruded during the Matuyama and Brunhes Chrons near McMurdo Sound, Antarctica, *Geochem. Geophys. Geosyst.*, *5*, G06H12, doi:10.1029/2003GC000656.

Tauxe, L., C. Luskin, P. Selkin, P. Gans, and A. Calvert (2004b), Paleomagnetic results from the Snake River Plain: Contribution to the time-averaged field global database, *Geochem. Geophys. Geosyst.*, *5*, Q08H13, doi:10.1029/2003GC000661.

Ubangoh, R. U., I. G. Pacca, and J. B. Nyobe (1998), Palaeomagnetism of continental sector of the Cameroon Volcanic Line West Africa, *Geophys. J. Int.*, *135*, 362–374.

Udagawa, S., H. Kitagawa, A. Gudmundsson, O. Hiroi, T. Koyaguchi, H. Tanaka, L. Kristjansson, and M. Kono (1999), Age and magnetism of lavas in Jokuldalur area, Eastern Iceland: Gilsa event revisited, *Phys. Earth Planet. Int.*, *115*, 147–171.

Vandamme, D. (1994), A new method to determine paleosecular variation, *Phys. Earth Planet. Int.*, *85*, 131–142.

Watkins, N. D., A. Hajash, and C. E. Abranson (1972), geomagnetic secular variation during the Brunhes epoch in the Indian and Atlantic Ocean regions, *Geophys. J. R. Astron. Soc.*, *28*(1), 1–25.

Watkins, N. D., I. McDougall, and L. Kristjansson (1977), Upper Miocene and Pliocene geomagnetic secular variation in the Borgarfjordur area of Western Iceland, *Geophys. J. R. Astron. Soc.*, *49*, 609–632.

Yamamoto, Y., K. Shimura1, H. Tsunakawa1, T. Kogiso, K. Uto, H. G. Barsczus, H. Oda, T. Yamazaki, and E. Kikawa (2002), Geomagnetic paleosecular variation for the past 5 Ma in the Society Islands, French Polynesia, *Earth Planets Space*, *54*, 797–802.

Zanella, E., and R. Lanza (1994), Remanent and induced magnetization in the volcanites of Lipari and Volcano (Aeolian Islands), *Ann. Geofis.*, *37*(5), 1149–1156.

Zanella, E., G. De Astis, P. Dellino, R. Lanza, and L. La Volpe (1999), Magnetic fabric and remanent magnetization of pyroclastic surge deposits from Vulcano (Aeolian Islands, Italy), *J. Volcanol. Geotherm. Res.*, *93*(3–4), 217–236.